Supporting Information

The Potential Use of Metal-Organic Framework/Ammonia Working Pairs in Adsorption Chillers

Zhilu Liu, [a,#] Guoliang An, [b,#] Xiaoxiao Xia, [a] Shaofei Wu, [b] Song Li, [a,*] and Liwei Wang [b,*]

[a] State Key Laboratory of Coal Combustion, School of Energy and Power Engineering, Huazhong University of Science and Technology, Wuhan 430074, China.
[b] Institute of Refrigeration and Cryogenics, Key Laboratory of Power Machinery and Engineering of MOE, Shanghai Jiao Tong University, Shanghai, 200240, China.
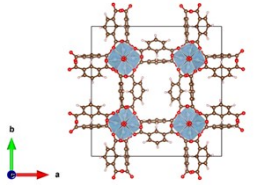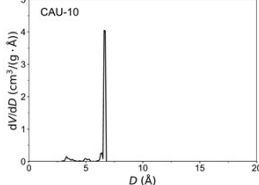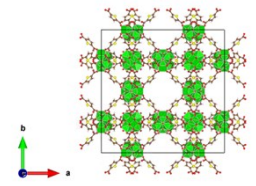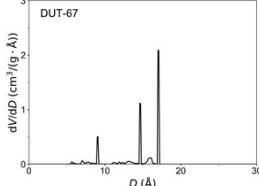[#] These authors contributed equally to this work.
* Corresponding author email: songli@hust.edu.cn; lwwang@sjtu.edu.cn.
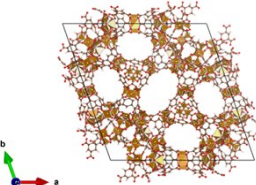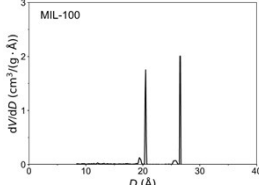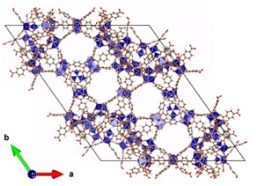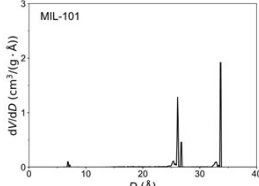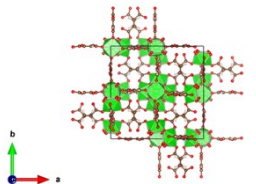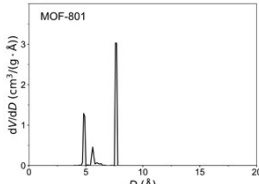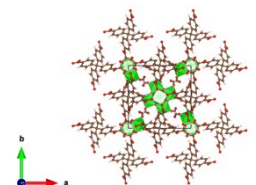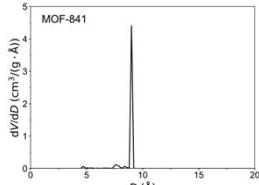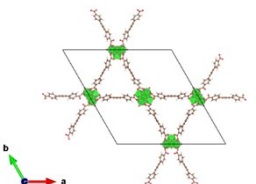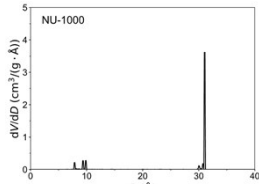
Table of Contents

S1. Grand Canonical Monte Carlo simulation methods

Table S1. The crystal structure of MOFs for GCMC simulation.

Number	Material	Metal	Density (g/cm³)	Crystal structure	PSD [a]
1	CAU-10 [1]	Al	1.125		
2	DUT-67 [2]	Zr	0.988		
3	MIL-100 [3]	Fe	0.697		
4	MIL-101 [4]	Cr	0.440		
5	MOF-801 [5]	Zr	1.742		
6	MOF-841 [5]	Zr	1.302		
7	NU-1000 [6]	Zr	0.442		

8	UiO-66 [7]	Zr	1.219		
9	ZIF-8 [8]	Zn	0.925		
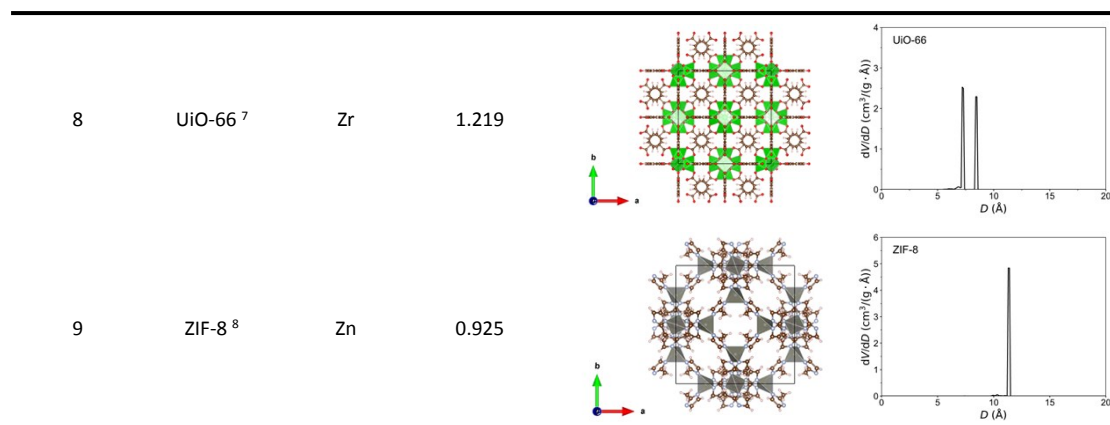
[a] The pore size distribution (PSD) was calculated using a probe with the ammonia radius of 1.3 Å in Zeo++ 0.3 [9].

Table S2. TraPPE force field parameters of ammonia

Number	(pseudo) Atom	Type	σ (Å)	ε/k_B (K)	q (e)
1	N	[N]-H_3	3.420	185.0	0
2	H	[H]-NH_2	0	0	0.410
3	M	[M]-NH_3	0	0	-1.230

3

S2. Computation details of cooling performance

Based on the basic thermodynamic cycle diagram of ACs in Figure 1, SCE is the energy transferred for cooling by working fluid (i.e. Q_{ev}). COP_C describes the thermodynamic efficiency of ACs that is defined as SCE divided by the total heat input to the system (i.e. Q_{input}, and it approximately equals Q_{des}). COP_C is defined

$$SCE = Q_{ev} \tag{Eq. S1}$$

$$COP_C = \frac{SCE}{Q_{input}} = \frac{Q_{ev}}{Q_{des}} \tag{Eq. S2}$$

Where Q_{ev} is the energy taken up in the evaporator, and Q_{input} is the heat energy from low-grade heat sources for desorption of adsorbent (Q_{des}).

$$Q_{ev} = \Delta W \Delta_{vap} H\left(T_{ev}\right) + \Delta W \int_{T_{con}}^{T_{ev}} C_p^{wf}\left(T\right) dT \tag{Eq. S3}$$

$$Q_{des} = Q_{\text{I-II}} + Q_{\text{II-III}}$$
$$= \left[\int_{T_{ads}}^{T_2} C_p^{ad}\left(T\right) dT + W_{max} \int_{T_{ads}}^{T_2} C_p^{wf}\left(T\right) dT \right] + \left[\int_{T_2}^{T_{des}} C_p^{ad}\left(T\right) dT + \int_{T_2}^{T_{des}} W\left(T\right) C_p^{wf}\left(T\right) dT + \int_{W_{max}}^{W_{min}} \Delta_{ads} H\left(W\right) dW \right] \tag{Eq. S4}$$

Here, in the calculation of Q_{ev}, $\Delta W \Delta_{ads} H\left(T_{ev}\right)$ and $\Delta W \int_{T_{con}}^{T_{ev}} C_p^{wf}(T) dT$ are latent heat and sensible heat taken up by the working fluid (ammonia in this work) in the evaporator. For the regeneration process of adsorbents (i.e. steps of I-II and II-III in Figure 1), $\int_{T_{ads}}^{T_2} C_p^{ad}(T) dT$ and $\int_{T_2}^{T_{des}} C_p^{ad}(T) dT$ are the energy required for the adsorbent bed temperature changing from T_{ads} to T_{des}. Notably, we neglected the impact of heat exchanger and only considered the effect of adsorbent. $W_{max} \int_{T_{ads}}^{T_2} C_p^{wf}(T) dT$ and $\int_{T_2}^{T_{des}} W(T) C_p^{ad}(T) dT$ are the energy required for the working fluid (ammonia in this work) temperature from T_{ads} to T_{des}. The last term $\int_{W_{max}}^{W_{min}} \Delta_{ads} H(W) dW$ is the heat adsorbed for ammonia desorption in the ACs system, where ΔW equals the difference of maximum water uptake (W_{max}) and minimum ammonia uptake (W_{min}).

$$\Delta W = W_{max} - W_{min} = W\left(T_{ads}, P_{ev}\right) - W\left(T_{des}, P_{con}\right) \tag{Eq. S5}$$

$\Delta_{vap} H(T_{ev})$ is the evaporation enthalpy of ammonia at T_{ev}, which can be calculated by fitting equation in *physical and chemical data*. [10]

$$\Delta_{vap} H = C1 \times \left(1 - \frac{T}{T_c}\right)^{C2 + C3 \times \frac{T}{T_c} + C4 \times \left(\frac{T}{T_c}\right)^2} \text{ (unit: kJ/mol)} \tag{Eq. S6}$$

T_c is critical temperature of ammonia, and other parameters were listed in Table S3.

Table S3. Parameters for the evaporation enthalpy of ammonia in Eq. S6

Temperature range (K)	C1	C2	C3	C4	T_c
195.41-405.65 K	31.523	0.3914	-0.2289	0.2309	405.65

$$\int_{W_{max}}^{W_{min}} \Delta_{ads}H(W)\mathrm{d}W$$

can be calculated by $\Delta W \times \Delta_{ads}H_{ave}$, where $\Delta_{ads}H_{ave}$ is the average value of isosteric heat of adsorption between W_{min} and W_{max}, which can be estimated by the following equation.

$$\Delta_{ads}H_{ave} = \frac{\int_{W_{min}}^{W_{max}} \Delta_{ads}H(W)\mathrm{d}W}{W_{max} - W_{min}} \approx \frac{\Delta_{ads}H(W_{max}) + \Delta_{ads}H(W_{min})}{2} \tag{Eq. S7}$$

In addition, C_p^{wf} and C_p^{ad} are the specific heat capacity of working fluid and adsorbent, respectively. They are considered to be constant (C_p varies slightly with temperature in fact) of 4.7 kJ/(kg·K) for ammonia [10] and 1 kJ/(kg·K) for MOFs (reasonable value for a variety of adsorbents) [11].

Then, the formula for calculating COP can be obtained by substitution and simplification.

$$SCE = \Delta W \left[\Delta_{vap}H(T_{ev}) - C_p^{wf}(T_{con} - T_{ev}) \right] \tag{Eq. S8}$$

$$COP_C = \frac{\Delta W \left[\Delta_{vap}H(T_{ev}) - C_p^{wf}(T_{con} - T_{ev}) \right]}{C_p^{ad}(T_{des} - T_{ads}) + C_p^{wf} \left[W_{max}(T_2 - T_{ads}) + \int_{T_2}^{T_{des}} W(T)\mathrm{d}T \right] - \Delta W \Delta_{ads}H_{ave}} \tag{Eq. S9}$$

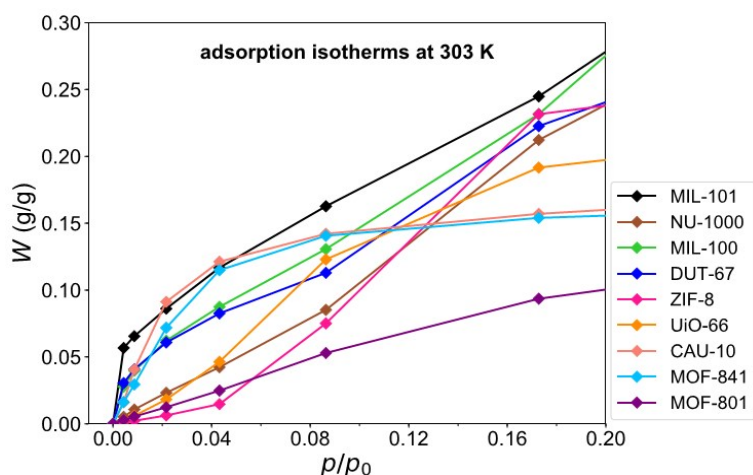## S3. GCMC simulation results of ammonia adsorption in MOFs

Figure S1. Ammonia adsorption isotherms of 9 adsorbents at 303 K and low relative pressure.

Table S4. The adsorption properties and cooling performances of nine adsorbents ranked by COP_C.

Rank	Material	ΔW		$\Delta_{ads}H_{ave}$	SCE		COP_C
		(g/g)	(g/cm³)	(kJ/kg)	(kJ/kg)	(10^{-3} kJ/m³)	
1	NU-1000	0.498	0.220	22.66	559.65	247.23	0.582
2	MIL-101	0.822	0.361	29.22	924.05	406.34	0.503
3	MIL-100	0.427	0.298	32.23	480.26	334.61	0.440
4	DUT-67	0.243	0.240	30.91	272.87	269.54	0.414
5	ZIF-8	0.200	0.185	32.22	225.21	208.21	0.395
6	UiO-66	0.144	0.175	34.45	161.69	197.11	0.348
7	MOF-801	0.100	0.174	32.97	112.15	195.35	0.333
8	CAU-10	0.078	0.088	36.24	87.72	98.72	0.265
9	MOF-841	0.060	0.079	35.74	67.97	88.47	0.235

Table S5. The reported cooling performance of nine adsorbents with water and ethanol as working fluids.

Number	Material	Water as working fluid			Ethanol as working fluid		
		Cooling conditions [a]	SCE or Q_{ev} [b]	COP_C	Cooling conditions [a]	SCE	COP_C
1	NU-1000	T_{des} = 393 K [12]	SCE = 86 kJ/kg	0.46	T_{des} = 393 K [12]	343 kJ/kg	0.67
2	MIL-101	T_{des} = 373 K [13]	SCE = 342 kJ/kg	0.76	T_{des} = 395 K [14]	464 kJ/kg	0.63
3	MIL-100	T_{des} = 373 K [13]	SCE = 363 kJ/kg	0.72	n.d.	n.d.	n.d.
4	DUT-67	T_{des} = 373 K [13]	SCE = 672 kJ/kg	0.79	T_{des} = 353 K [15]	n.d.	0.75
5	ZIF-8	T_{des} = 373 K [13]	SCE = 2.22 kJ/kg	0.03	T_{des} = 395 K [14]	183 kJ/kg	0.62
6	UiO-66	T_{des} = 393 K [12]	SCE = 96 kJ/kg	0.48	T_{des} = 393 K [12]	410 kJ/kg	0.61
7	MOF-801	T_{des} = 373 K [11]	Q_{ev} = 280 kWh/m³	0.65	n.d.	n.d.	n.d.
8	CAU-10	T_{des} = 373 K [11]	Q_{ev} = 245 kWh/m³	0.70	n.d.	n.d.	n.d.
9	MOF-841	T_{des} = 373 K [11]	Q_{ev} = 330 kWh/m³	0.81	n.d.	n.d.	n.d.

[a] The cooling working conditions in ACs: T_{ev} = 283 K, T_{con} = T_{ads} = 303 K.

[b] Q_{ev} is energy taken up by the evaporator from de Lange et. al.

S4. The experimental methods and results

S4.1. Experiment Methods

S4.1.1. Synthesis

NU-1000. Chemicals for synthesizing NU-1000 are listed as follows. Zirconyl chloride octahydrate ($ZrOCl_2 \cdot 8H_2O$, 99.9%) and benzoic acid (99.9%) were purchased from Shanghai Aladdin Bio-Chem Technology Co. Ltd. Tetraethyl 4,4',4'',4'''-(pyrene-1,3,6,8-tetrayl) tetrabenzoic acid (H_4TBAPy, 98 %) was purchased from Zhengzhou Alfachem Co. Ltd. N,N-dimethylformamide (DMF), hydrochloric acid (HCl) and acetone were provided by Sinopharm Chemical Reagent Co., Ltd. (AR). All chemicals were used without further purification.

NU-1000(Zr) was synthesized based on previous report.[16] $ZrOCl_2 \cdot 8H_2O$ (1.94 g, 6.02 mmol) and benzoic acid (54 g, 0.442 mol) were dissolved in DMF (120 mL, 1.55 mol) by using ultrasound, and then the solution was maintained at 373 K for 1 h. In the meantime, H_4TBAPy (0.8 g, 1.17 mmol) was added into 40 mL DMF using sonication to evenly suspend the H_4TBAPy in the solvent, which was then placed in a 373 K oven for 1 h. After that, when the suspension became a clear solution, the two solutions were mixed and transferred to a 500 mL round-bottomed flask, which was kept at 393 K under static conditions for 16 h. The precipitates were isolated by centrifugation, and then washed with fresh DMF for three times, in which the precipitate was soaked in DMF for 2 h each time. The solution obtained was transferred to a 500 mL beaker with 260 mL of DMF and 10 ml of 8 M HCl aqueous solution was added, which was then placed in a 373 K oven for 12 h. The precipitates were isolated by centrifugation and washed by fresh DMF for three times similarly as above-mentioned. Then, the precipitates were washed by fresh acetone for three times and the precipitate was soaked for 12 h each time. Finally, the solids were dried in air at 353 K for 12 h, and then dried under vacuum at 353 K for 12 h.

MIL-101. Chemicals for synthesizing MIL-101 are listed as follows. Chromium(III) nitrate nonahydrate ($Cr(NO_3)_3 \cdot 9H_2O$, 99 %) and terephthalic acid (H_2BDC, 99 %) were from Shanghai Aladdin Bio-Chem Technology Co., Ltd. Glacial acetic acid (AR), ethanol (AR) and N,N-dimethylformamide (DMF, AR) were purchased from Sinopharm Chemical Reagent Co., Ltd. All chemicals were used without further purification.

MIL-101(Cr) was synthesized based on previous report with a slight modification. [17] 4.00 g (10 mmol) $Cr(NO_3)_3 \cdot 9H_2O$ and 1.66 g (10 mmol) H_2BDC were added in 50 mL deionized water. Then, 0.58 mL glacial acetic acid was added. After sonicating for 30 minutes at room temperature, the reactant mixture was transferred into a 100 mL capacity Teflon-lined autoclave and heated at 493 K for 8 h. Next, the reactor was cooled down gradually to room temperature. Then, the green solid obtained was washed successively with deionized water, DMF and ethanol. Finally, the obtained solid was dried at 423 K under vacuum for 12 h.

S4.1.2 Characterization analysis

Powder X-ray diffraction (PXRD) data were obtained from a PANalytical X'Pert X-ray diffractometer by Cu Kα (λ = 1.540598 Å) radiation with a step size of 0.01313° from 2 to 15° in 2θ. **Scanning electron microscope (SEM)** images were conducted on a Quanta 200 SEM instrument. Scanning was carried out on the samples previously dried and sputter-coated with a gold layer at an accelerating voltage of 30 kV. Nitrogen (N_2) adsorption isotherms were measured at 77 K on a Quantachrome Autosorb-iQ2 gas analyzer. Samples were activated at 393 K for 24 h under vacuum before measurement. Then, the **surface area (S_a)** was estimated by Brunauer-Emmett-Teller (BET) equation used to fit the data at relative pressure between 0.08 and 0.25 on N_2 adsorption isotherm. The **pore volume (V_p)** and **pore size distribution (PSD)** were obtained using t-plot and non-local density functional theory methods, respectively.
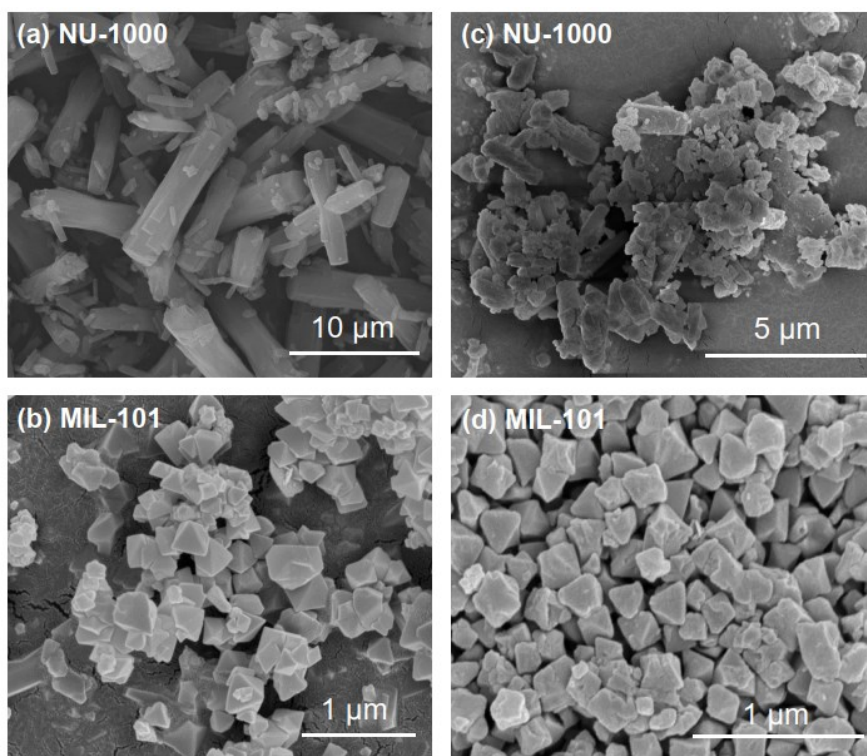
S4.2 Experiment results

Figure S2. The SEM image of (a) NU-1000 and (b) MIL-101 before ammonia adsorption, (c) NU-1000 and (d) MIL-101 after ammonia adsorption.

Table S6. The structural characteristics of NU-1000 and MIL-101(Cr) before and after ammonia adsorption.

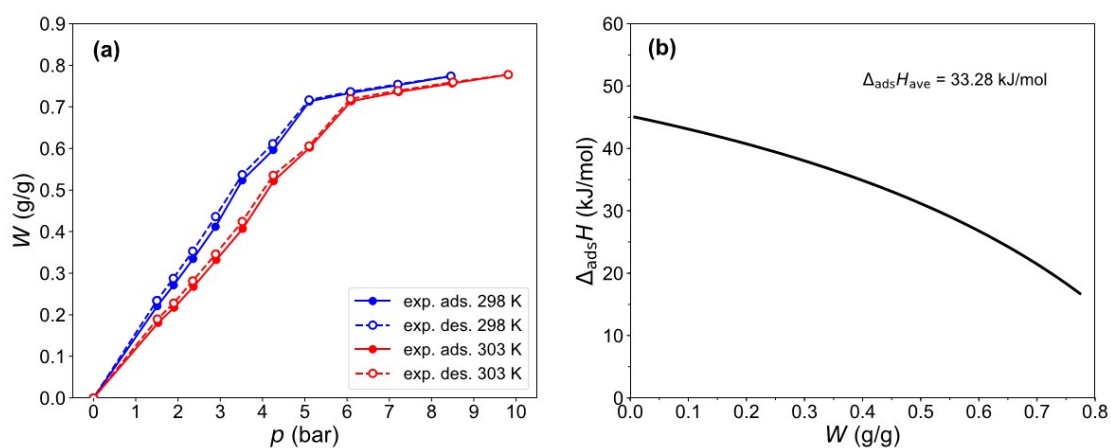| Materials	Before or after NH$_3$ adsorption	BET surface area (S_a, m^2/g)	Total pore volume (V_p, cm^3/g)	Pore size (nm)
NU-1000	Before	2361	1.49	1.06/3.55
	After	296	0.18	—
MIL-101	Before	3358	2.09	2.58/3.18
	After	2017	1.43	2.58/3.18

Figure S3. (a) The experimental adsorption isotherms of MIL-101 at 298 K and 303 K. (b) The heat of adsorption of MIL-101 for NH$_3$ adsorption calculated by Clausius-Clapeyron equation based on the experimental adsorption isotherms.

References

1. D. Fröhlich, E. Pantatosaki, P. D. Kolokathis, K. Markey, H. Reinsch, M. Baumgartner, M. A. van der Veen, D. E. De Vos, N. Stock, G. K. Papadopoulos, S. K. Henninger and C. Janiak, *J. Mater. Chem. A*, 2016, **4**, 11859-11869.

2. V. Bon, I. Senkovska, I. A. Baburin and S. Kaskel, *Cryst. Growth Des.*, 2013, **13**, 1231-1237.

3. P. Horcajada, S. Surble, C. Serre, D. Y. Hong, Y. K. Seo, J. S. Chang, J. M. Greneche, I. Margiolaki and G. Ferey, *Chem. Commun.*, 2007, **27**, 2820-2822.

4. G. Ferey, C. Mellot-Draznieks, C. Serre, F. Millange, J. Dutour, S. Surble and I. Margiolaki, *Science*, 2005, **309**, 2040-2042.

5. H. Furukawa, F. Gandara, Y. B. Zhang, J. Jiang, W. L. Queen, M. R. Hudson and O. M. Yaghi, *J. Am. Chem. Soc.*, 2014, **136**, 4369-4381.

6. J. E. Mondloch, W. Bury, D. Fairen-Jimenez, S. Kwon, E. J. DeMarco, M. H. Weston, A. A. Sarjeant, S. T. Nguyen, P. C. Stair, R. Q. Snurr, O. K. Farha and J. T. Hupp, *J. Am. Chem. Soc.*, 2013, **135**, 10294-10297.

7. J. H. Cavka, S. Jakobsen, U. Olsbye, N. Guillou, C. Lamberti, S. Bordiga and K. P. Lillerud, *J. Am. Chem. Soc.*, 2008, **130**, 13850-13851.

8. K. S. Park, Z. Ni, A. P. Cote, J. Y. Choi, R. D. Huang, F. J. Uribe-Romo, H. K. Chae, M. O'Keeffe and O. M. Yaghi, *Proc. Natl. Acad. Sci. U.S.A.*, 2006, **103**, 10186-10191.

9. T. F. Willems, C. H. Rycroft, M. Kazi, J. C. Meza and M. Haranczyk, *Microporous Mesoporous Mater.*, 2012, **149**, 134-141.

10. R. H. Perry, *Perry's chemical engineers' handbook*, 1984, 7.

11. M. F. de Lange, K. J. Verouden, T. J. Vlugt, J. Gascon and F. Kapteijn, *Chem. Rev.*, 2015, **115**, 12205-12250.

12. X. Xia, M. Cao, Z. Liu, W. Li and S. Li, *Chem. Eng. Sci.*, 2019, **204**, 48-58.

13. Z. Liu, W. Li, P. Z. Moghadamc and S. Li, *Sustainable Energy & Fuels*, 2021.

14. X. Xia, Z. Liu and S. Li, *Appl. Therm. Eng.*, 2020, **176**, 115442.

15. W. Li, X. Xia, M. Cao and S. Li, *J. Mater. Chem. A*, 2019, **7**, 7470-7479.

16. T. C. Wang, N. A. Vermeulen, I. S. Kim, A. B. Martinson, J. F. Stoddart, J. T. Hupp and O. K. Farha, *Nat. Protoc.*, 2016, **11**, 149-162.

17. P. B. S. Rallapalli, M. C. Raj, S. Senthilkumar, R. S. Somani and H. C. Bajaj, *Environ. Prog. Sustainable Energy*, 2016, **35**, 461-468.